11th International Conference on Vibration Problems
Z. Dimitrovová *etal.* (eds.)
Lisbon, Portugal, 9–12 September 2013

# EXPERIMENTAL INVESTIGATION OF THE THREE DIMENSIONAL VIBRATION OF SMALL LIGHTWEIGHT OBJECTS

**Sebastian Ihrle*, Albrecht Eiber, Peter Eberhard**

Institute of Engineering and Computational Mechanics, University of Stuttgart,
Pfaffenwaldring 9, 70550 Stuttgart, Germany
[sebastian.ihrle, albrecht.eiber, peter.eberhard]@itm.uni-stuttgart.de

**Keywords:** Three Dimensional Vibration, Small Lightweight Objects, Biomechanics, Human Hearing.

**Abstract.** *In this article an experimental setup for measuring spatial vibrations of small, lightweight objects is presented. To avoid mass-loading effects caused by conventional transducers, nonintrusive measurements with Laser Doppler Vibrometers (LDVs) are performed. The spatial vibration of a single point is obtained using three coupled single LDVs. The optical axes of the LDVs are orientated linear not in one plane and the velocity vector is calculated from the three laser signals. Electrically driven translation stages are used to adjust the position of the measurement point on the object. A biological joint connecting two ossicles of the human middle ear is investigated. One of the ossicles is excited by an electrodynamic shaker. The velocity vector of several points on both ossicles is measured and the relative motion between the ossicles, which characterizes the joint, is reconstructed. With the described measurement system, the complex vibration pattern of a small structure can be reconstructed.*

## 1 INTRODUCTION

To obtain the dynamics of small lightweight objects it is essential to avoid undefined loads caused by the measurement system. Furthermore, the measurement system has to deal with the small dimensions of the specimen. Laser Doppler Vibrometers (LDVs) are ideal tools for this task, since they allow nonintrusive, high spatial resolution measurements even on microstructures. The performance of LDV measurements is demonstrated by its application in many engineering problems as summarized in [1].

In our research group the dynamics of human hearing is investigated. With vibration amplitudes in the lower micrometer range, the LDV has become the standard tool for evaluation of the vibrations in human hearing. In a previous study [2], the influence of rotational components of the stapes ossicle to hearing impression was investigated. The results show, that the complete spatial motion has to be considered when examining human hearing. With a single LDV only the component in the laser line-of-sight is captured. To overcome this drawback and obtain the complete spatial information we build a measurement setup consisting of three LDV units.

In this paper we describe our measurement system in detail and evaluate its performance on two benchmark setups. In addition, we present our measurements of the spatial movement of artificial osssicles, mimicking those of the human middle ear.

## 2 MEASUREMENT SYSTEM

With the measurement setup shown in Fig. 1 the spatial velocity and displacement vector at several points on an objects surface is measured. By combining the signals of three independent LDVs the spatial velocity and displacement vector can be retrieved. The laser spots are aligned in a triangular shape, not focusing on a single point to minimize the crosstalk between the three laser signals. The angles $\eta, \zeta, \delta$ define the orientation of the laser beams. They are given by the mounting and used to calculate the spatial vibration. In this work, the rigid body motion of artificial ossicles, mimicking those of the human middle ear, is obtained from measurements at several non collinear points. This is based on the assumption that elastic deformations of the ossicles can be neglected compared to the rigid body motions.

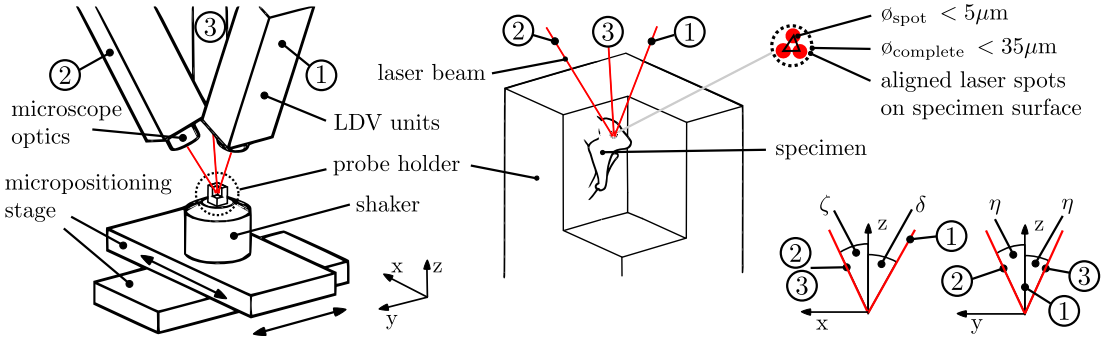


Figure 1: Schematic of the measurement setup. The position of the laser spots on the specimen surface is adjusted using the micropositioning stages.

### 2.1 Velocity and displacement measurement

Three conventional fiber LDVs (Polytec OFV-534, Waldbronn, Germany) are orientated along the edges of a tetrahedron aiming at a common measurement point. Each one is equipped with microscope optics to decrease the spot diameter. The position of the spots is controlled

using the integrated cameras of the vibrometers. To minimize the crosstalk between the laser signals, the laser spots are aligned in a triangular shape, but are not focusing on a single point. Generally speaking, extensive crosstalk leads to signal failure with a fluctuating noise level in the recorded signal. With the diameter of the total measurement spot being approximately 35 $\mu$m, the spatial resolution is fine enough to measure very small objects.

The laser beams are aligned in different directions which are orientated oblique to the objects surface. Since every LDV unit needs a certain amount of backscattered light, the surface of the specimen must be rough. We use therefore glass beads and a custom made white pigment paste to improve the signal levels.

### 2.2 Positioning of the measurement point

To reconstruct the motion of the object surface an accurate positioning of the laser spots on the specimen surface is necessary. Here, the x-y-position of the object is changed using electrically driven micropositioning stages (Physik Instrumente M-126.CG1, Karlsruhe, Germany). Each one has a bidirectional repeatability of 2.5 $\mu$m, which is smaller than the spot diameter of the laser beams. To automatise the measurement the user can define these positions prior to the measurement.

In case of a curved surface, the laser beams are refocused at the different measurement points to ensure that enough laser light is backscattered to the LDVs. Therefore, the mounting of the LDVs can be translated in z-direction with a manual micrometer-driven translational stage. A similar setup was used in [3] and [4] for obtaining one-dimensional velocity and displacement components of microstructures.

### 2.3 Excitation and data aquisition

We use two different mechanisms for exciting the specimen: a dynamic and a quasi-static excitation. In case of the dynamic one, the specimen is excited by an electrodynamic shaker using different test signals, e.g. sweep and band-limited white noise. In case of the quasi-static excitation, the specimen is excited by applying a quasi-static force while measuring the resulting displacement subsequently at different points.

The signal processing, i.e. the generation of the excitation signal, the control of the translational stages and the recording of the measurement data is done within a realtime environment (dSpace, Paderborn, Germany). The system is controlled by an external computer using MATLAB.

## 3 MEASUREMENT PROCEDURE

The specimen is mounted on an acrylic probe holder (15x15x18 mm$^3$, 5.8 g), see Fig. 1. The probe holder has three threaded holes orientated perpendicular to each other. Depending on the type of excitation the specimen is mounted to a shaker, using one of this threaded holes or clamped with a small vice. Generally, LDV measurements were performed subsequently at several points on the specimen surface with the excitation retained unchanged. By combining those measurements the deformation of the specimen surface or its rigid body motion is calculated.

### 3.1 Dynamic measurement

The vibration of the specimen is measured for three perpendicular directions of excitation. The specimen is excited by an electrodynamic mini-shaker (Brüel&Kjær 4810, Nærum, Denmark). The probe holder is mounted to the shaker by a screw. The shaker is driven by the signal

generated by the real-time computer and amplified by a Brüel&Kjær type 2718 amplifier.

For each excitation direction the following measurement procedure is repeated: The transducer is placed on the displacement table with the axes of the probe holder aligned along the axis of the micropositioning stages. A reference point on the object surface is chosen and additional LDV measurement points are defined relative to this reference point. The data acquisition parameters, e.g. sampling rate, number of samples per block and LDV sensitivities are set within MATLAB. After defining the excitation signal and the number of repetitions the semi-automatic measurement is started. When the position of the laser spots is changed, the user adjusts the focus manually and send a command to the measurement system. Finally, the data is transferred from the real-time computer to the computer for data processing.

### 3.2 Quasi-static measurement

The specimen is excited by a stylus (ball shaped tip, diameter 0.5 mm) connected to a load cell (Kyowa LVS-20 GA, Chofu, Japan; with nominal force 200 mN). The load cell is driven by a micropositioning stage in direction of the long axis of the stylus. The time-displacement profile of the translational stage is defined prior to the measurement. The spatial displacement at different measurement points on the specimen surface is measured subsequently, retaining both the time-displacement profile and the force application point unchanged. At the beginning of each measurement, the translational stage is driven manually towards the specimen until a slight change of the force level is detected. The stylus is then moved backwards until the force level drops to zero and the measurement is started.

We use a low-frequency (0.1 Hz) sinusoidal excitation with displacement amplitudes in between 90 and 190 $\mu$m. To characterize the relaxation of the system, additional measurements with a displacement step profile were performed.

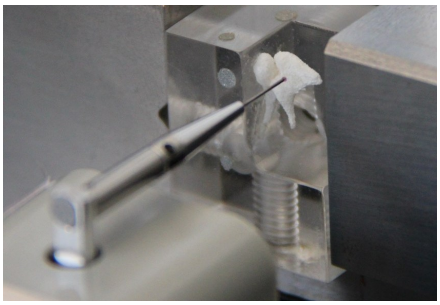

Figure 2: Probe holder clamped in a small vice.

### 3.3 Reconstruction of the rigid body motion

Using the spatial velocity or displacement of at minimum three non collinear points, the rigid body motion of the structure is calculated. Figure 3 shows a rigid body in its initial configuration at time $t_0 = 0$ and at time $t_1$.

The displacement $\mathbf{u}_i^{(I)}(t_1)$ of a point $P_i$ described in a fixed reference frame $K^I$ is calculated as

$$\mathbf{u}_i^{(I)}(t_1) = \tilde{\mathbf{S}}^{(I)}(t_1)\mathbf{a}_i^{(1)} + \mathbf{u}_{K^1}^{(I)}(t_1) \quad \text{with} \quad \tilde{\mathbf{S}}^{(I)}(t_1) = \begin{bmatrix} 0 & -\gamma(t_1) & \beta(t_1) \\ \gamma(t_1) & 0 & -\alpha(t_1) \\ -\beta(t_1) & \alpha(t_1) & 0 \end{bmatrix}. \qquad (1)$$

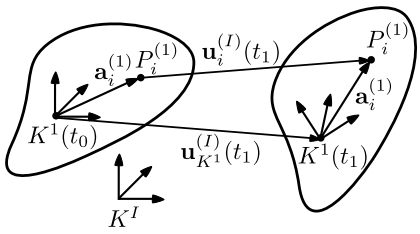


Figure 3: Motion of a free rigid body. The displacement $\mathbf{u}_i^{(I)}(t_1)$ of a point $P_i$ is measured by the LDV system.

Hereby $\tilde{\mathbf{S}}^{(I)}(t_1)$ denotes the linearized rotation matrix from the initial configuration to the configuration at time $t_1$, $\mathbf{a}_i^{(1)}$ is the coordinate of $P_i$ in the body fixed frame $K^1$. The displacement of the frame $K_1$ is given by $\mathbf{u}_{K^1}^{(I)}(t_1)$.

The position and orientation of the rigid body can be described using the set of generalized coordinates

$$\mathbf{q}(t_1) = \begin{bmatrix} u_{K^1,x}^{(I)}(t_1) & u_{K^1,y}^{(I)}(t_1) & u_{K^1,z}^{(I)}(t_1) & \alpha(t_1) & \beta(t_1) & \gamma(t_1) \end{bmatrix}^{\mathrm{T}}. \tag{2}$$

The displacements $\mathbf{u}_i^{(I)}(t_1)$ measured at $n \geq 3$ non collinear points are combined to the overdetermined system of equations

$$\begin{bmatrix} \mathbf{u}_1^{(I)}(t_1) \\ \vdots \\ \mathbf{u}_n^{(I)}(t_1) \end{bmatrix} = \begin{bmatrix} \mathbf{A}_1 \\ \vdots \\ \mathbf{A}_n \end{bmatrix} \mathbf{q}(t_1) \quad \text{with} \quad \mathbf{A}_i = \begin{bmatrix} 1 & 0 & 0 & 0 & a_{z,i} & -a_{y,i} \\ 0 & 1 & 0 & -a_{z,i} & 0 & a_{x,i} \\ 1 & 0 & 0 & a_{y,i} & -a_{x,i} & 0 \end{bmatrix}. \tag{3}$$

The generalized coordinates $\mathbf{q}(t_1)$ are calculated by solving Eq. (3) with the method of minimizing the least square error.

## 4 VALIDATION OF THE MEASUREMENT SETUP

### 4.1 Dynamic measurement

The probe holder is excited with a shaker and the spatial velocity is measured at a point on the probe holder. Afterwards a second measurement is performed, using a single LDV orientated perpendicular to the probe holder in z-direction. Figure 4(a) shows a foto of the measurement setup.

The amplitude of the transfer function describing the velocity of the measurement point per volt of the input excitation of both measurements is compared in Fig. 4(b). There is no significant difference in the z-component. The transfer function is computed from the signal of the three independent LDVs. Hence the setup is capable to capture the correct spatial component. It is possible to identify a resonance at 1.3 kHz with a significant amount of in-plane motion caused by bending of the shaker rod.

### 4.2 Static measurement

One of the translational stages carrying the probe holder is driven by a low-frequent sinusoidal time-displacement profile. The displacement of a point on the probe holder is measured and compared to the data obtained from the incremental encoder of the translational stage. The stylus is not touching the specimen.

Figure 5 shows a comparison of both signals. The translational stage orientated in y-direction is driven with an amplitude of 300 $\mu$m. The spatial displacement obtained from the LDVs shows

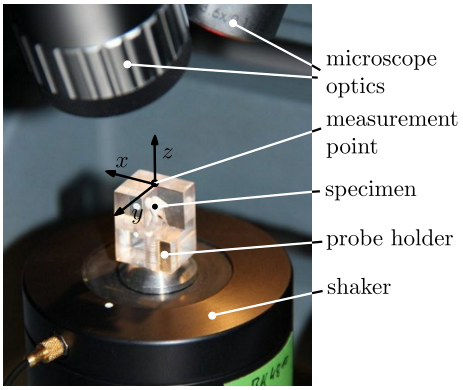


(a) Dynamic excitation of the probe holder.

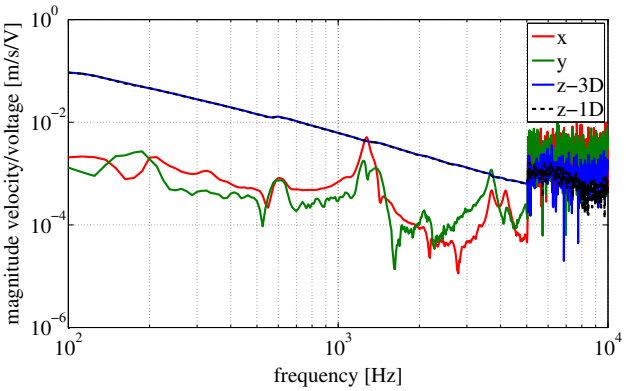


(b) Magnitude of the transfer function describing the spatial velocity of the measurement point.

Figure 4: The probe holder was excited with a shaker driven by band-limited white noise (100-5000 Hz). The z-component was measured twice, using the 3D system and a 1D-LDV orientated perpendicular to the x-y-plane. There is no significant difference between both signals in the transfer function.

a slight fluctuation of the maximum values mainly caused by the tolerance of the translational stage. The values of the x- and z-component are proportional to the error of the measurement setup including possible misalignment of the probe holder. Both are quite small compared to the y-component.

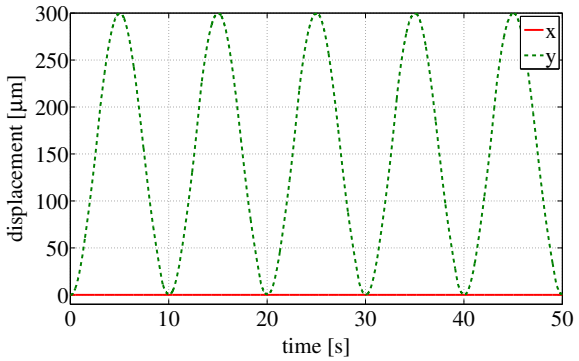


(a) Displacement of translational stage.

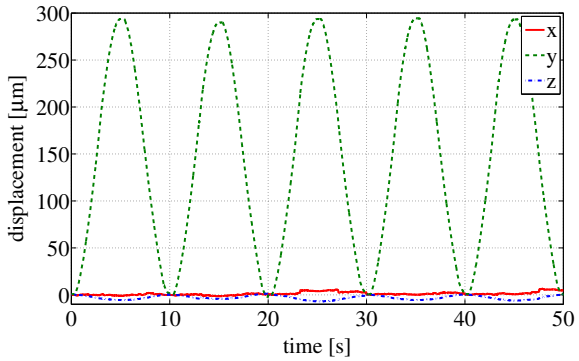


(b) Displacement obtained from the 3D-LDV system.

Figure 5: Comparison of the stage displacement obtained from the incremental encoder and the 3D-LDV system. The translational stage was driven in y-direction by a low-frequency (0.1 Hz) sinusoidal time-displacement profile.

## 5 APPLICATION

The measurement setup is used to investigate the behavior of a biological joint connecting two ossicles of the human middle ear - namely the malleus and incus bones. To examine the contribution of the incudo-malleolar joint (IMJ) to the sound transmission, human temporal bone experiments are performed. Therefore, preliminary measurements using artificial ossicles were conducted in order to prepare both, the measurement setup and the data analysis. Based on micro-computer tomography (micro-ct) data of human specimen, artificial ossicles matching the specimen geometry were created using selective laser sintering. The artificial malleus and incus were orientated to each other according to the micro-ct data and connected by rubber cement forming a flexible bond. Figure 2 shows a foto of the artificial ossicles, the malleus is

glued to the probe holder.

### 5.1 Dynamic excitation

Measurements are performed with the probe holder orientated in three different directions. The velocity is measured at points on the specimen and the probe holder. For comparison of the results they are transformed from the LDV frame to a specimen frame. The alignment of the specimen frame and the LDV frame for a variant of the probe orientation is shown in Fig. 6(a). The excitation direction is always pointing in z-direction of the LDV frame. The $\tilde{z}$-axis of the specimen frame is orienated along a line connecting the malleus head with its tip. The $\tilde{x}$-axis is orientated along the anterior processus of the malleus.

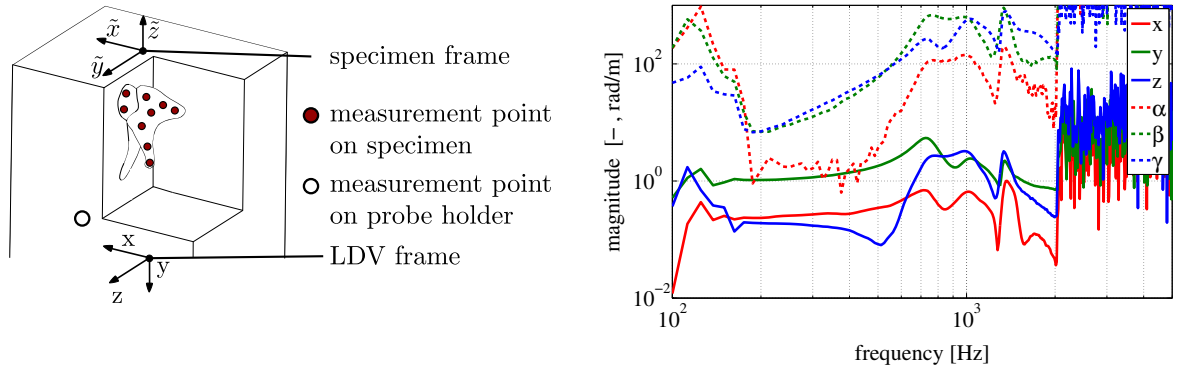


(a) Alignment of the specimen frame and position of the measurement points with the specimen excited in $\tilde{y}$ direction.

(b) Magnitude of the transfer function between the z-vibration of the malleus and the generalized coordinates of the incus.

Figure 6: Vibration excitation of the specimen in $\tilde{y}$ direction. The malleus is rigidly connected to the probe holder. The incus exhibits a spatial movement with two prominent resonance peaks at 725 and 925 Hz.

The rubber cement mimics the nonlinear stiffness characteristic of the IMJ. Hence the shaker is driven randomly by band-limited white noise (200-2000 kHz; -46 dB PSD). The frequency response function between the voltage supplied to the amplifier of the shaker and the velocity of the measurement point is determined with the $\hat{H}_1$ estimator as described in [5]. Therefore, Welch's method [6] is applied to calculate the average power spectra using a Hanning window function with 75% overlap. The transfer function of a point on the malleus and another one on the probe holder shows no significant difference. This verifies that both are rigidly connected. The results of several points on the incus surface are used to calculate the transfer function from the z-component of the malleus to the generalized coordinates of the incus. The generalized coordinates $\mathbf{q}_{\text{Inc}} = [x\, y\, z\, \alpha\, \beta\, \gamma]$ are expressed in a coordinate system located at the center of gravity of the incus and orientated like the specimen frame. Fig. 6(b) shows the magnitude of this transfer function.

At frequencies below 300 Hz there is no significant relative motion between both ossicles. As the frequency rises, the relative motion does too. Since the malleus is fixed at the probe holder its vibration is translational, whereas the incus exhibits a complex spatial vibration. The relative motion of the incus at two prominent resonance frequencies is visualised by the trajectories drawn in Fig. 7. In both cases the relative motion of the incus is not orientated along the axis of excitation. At 725 Hz the incus moves along the neck of the malleus, at 1025 Hz it vibrates perpendicular to it. The elliptic form of the trajectories is caused by the rotational motion and increases above frequencies of 300 Hz. This increase of rotational motion can also be seen in

the transfer function since the magnitudes of the generalized angles, describing the orientation of the incus, are also rising.

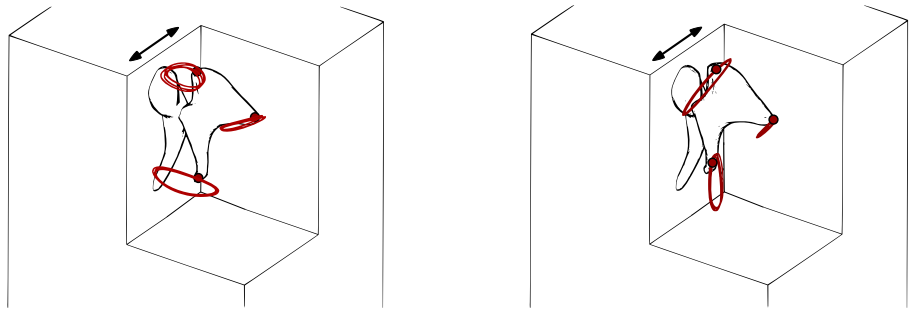

(a) $f = 725$ Hz. (b) $f = 1025$ Hz.

Figure 7: Visualisation of the relative motion of the incus when the probe holder is excited in the marked direction.

### 5.2 Static excitation

The incus is excited at several points by a stylus applying a low frequency sinusoidal excitation (0.1 Hz) with a maximum displacement of 120 $\mu$m. The spatial displacement is measured at several points on the incus surface. Figure 8 shows the data obtained from a single measurement with a force applied on the short process of the incus. In case of the complete measurement, the displacement measurement is repeated at different points on the incus, with the excitation signal and the force application poined retained unchanged.

The fusion of the load cell data, the encoder information of the translational stages and the 3D-LDV system allows a detailed characterization of the artificial IMJ. The force deflection curves are nonlinear with prominent changes of its slope at different displacement levels. Its characteristic is degressive at the beginning, switching to a progressive one at 2/3 of the displacement amplitude. A possible reason is a contact of both ossicles applying a kinematical constraint caused by the saddle shaped geometry of the IMJ.

### 5.3 CONCLUSION AND OUTLOOK

We presented a setup capable of measuring the spatial velocity and displacement of small lightweight objects. To validate our system, measurements have been carried on two benchmark setups.

Measurements on artificial ossicles were performed. The rigid body motion was calculated from the spatial movement at several points on the specimen surface. The incus exhibited a complex spatial motion which depended on the frequency and orientation of the excitation. Therefore, capturing the three-dimensional movement is essential to describe the IMJ adequately. The semi-automatic adjustment of the laser beam with the definition of the measurement positions in a pre-measurement step reduces the measurement time, helping to prevent a biological specimen from drying out.

Based on these results next measurements of human temporal bones are performed. Figure 9 shows a foto of a specimen attached to the probe holder and the raw data of the LDVs of a single measurement. With the data obtained from those measurements we will derive parameters to improve our elastic multibody system of the human middle ear presented in [7].

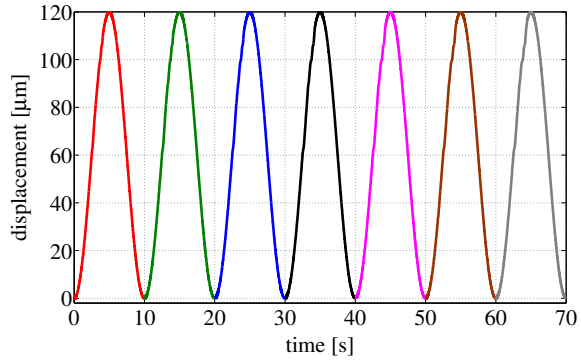


(a) Displacement excitation applied to the translational stage.

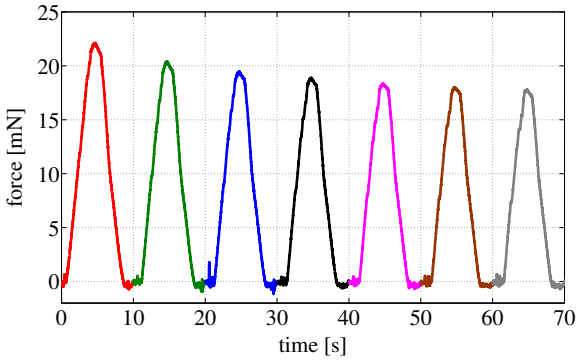


(b) Raw data obtained from the load cell. The peak value decreases due to preconditioning.

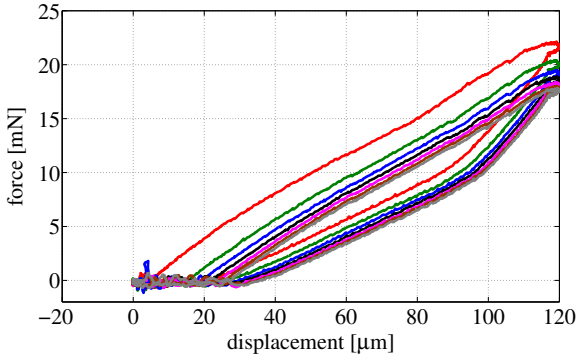


(c) Force deflection curve showing the typical properties of soft tissue: nonlinearity, hysteresis and preconditioning.

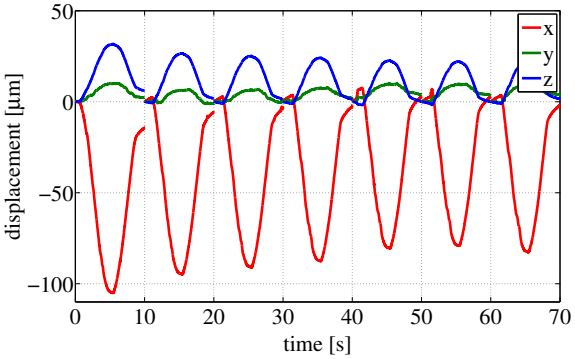


(d) Spatial displacement of the 3D-LDV measurement point. The incremental encoder of the LDV units is reset at the end of each cycle.

Figure 8: Data obtained from a measurement with a force applied in negative x-direction at the short processus of incus. Each cycle of the sinousoidal excitation profile is plotted using a different color. The 3D-LDV measurement point located on the back of the incus exhibits a spatial motion.

(a) Human temporal bone attached to the probe holder.

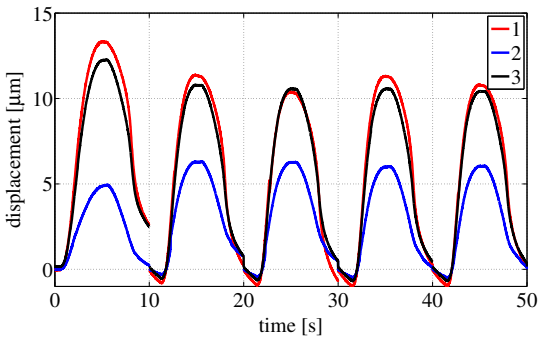


(b) Raw data of the three LDVs.

Figure 9: Measurements of human temporal bones.

## REFERENCES

[1] P. Castellini, M. Martarelli, and E. Tomasini, Laser doppler vibrometry: Development of advanced solutions answering to technology's needs, *Mechanical Systems and Signal Processing*, **20**, 1265–1285, 2006.

[2] A. Eiber, A. M. Huber, M. Lauxmann, M. Chatzimichalis, D. Sequeira, and J. H. Sim, Contribution of complex stapes motion to cochlea activation, *Hearing Research*, **284**, 82 – 92, 2012.

[3] M. M. Guillemot-Amadei, L. Petit, L. Lebrun, R. Briot, and P. Gonnard, A non-contact measurement technique for piezoelectric transducers, *Measurement Science and Technology*, **6**, 458–466, 1995.

[4] J. Burdess, A. Harris, D. Wood, R. Pitcher, and D. Glennie, A system for the dynamic characterization of microstructures, *Journal of Microelectromechanical Systems*, **6**, 322–328, 1997.

[5] K. G. McConnell and P. S. Varoto, *Vibration testing: theory and practice*. New York: John Wiley & Sons, 2008.

[6] P. Welch, The use of fast fourier transform for the estimation of power spectra: a method based on time averaging over short, modified periodograms, *IEEE Transactions Audio and Electroacoustics*, **15**, 70–73, 1967.

[7] S. Ihrle, M. Lauxmann, A. Eiber, and P. Eberhard, Nonlinear modelling of the middle ear as an elastic multibody system-applying model order reduction to acousto-structural coupled systems, *Journal of Computational and Applied Mathematics*, **246**, 18–26, 2012.